

Novel Vibrational Proteins

Yage Chen,[†] Zhiliang Huang,[†] Erli Cai,[†] Shuchen Zhong, Haozheng Li, Wei Ju, Jie Yang, Wei Chen,*
Chun Tang* and Ping Wang*Cite This: *Anal. Chem.* 2024, 96, 16481–16486

Read Online

ACCESS |



Metrics & More

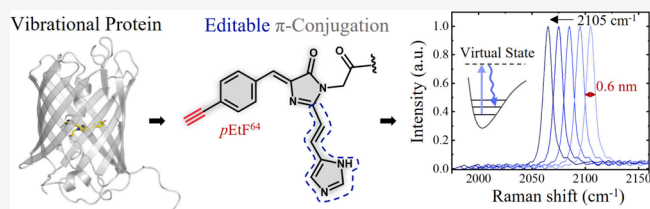


Article Recommendations



Supporting Information

ABSTRACT: Genetically encoded green fluorescent protein (GFP) and its brighter and redder variants have tremendously revolutionized modern molecular biology and life science by enabling direct visualization of gene regulated protein functions on microscopic and nanoscopic scales. However, the current fluorescent proteins (FPs) only emit a few colors with an emission width of about 30–50 nm. Here, we engineer novel vibrational proteins (VPs) that undergo much finer vibrational transitions and emit rather narrow vibrational spectra (0.1–0.3 nm, roughly 3–10 cm^{-1}). In response to an amber stop codon (UAG), a terminal alkyne bearing an unnatural amino acid (UAA, *p*EtF) is directly incorporated in place of Tyr64 in the chromophore of pr-Kaede by genetic code expansion. Essentially, the UAA64 further conjugates into a large π system with the contiguous two editable amino acid residues (His63 and Gly65), resulting in a programmable Raman resonance shift of the embedded alkyne. In the proof-of-concept experiment, we constructed a series of novel *p*EtF-VP mutants and observed fine Raman shifts of the alkynyl group in different chromophores. The genetically encoded novel VPs, could potentially label tens of proteins in the future.



INTRODUCTION

Proteins that can emit fluorescence are nature's magic gifts.^{1,2} Over the past decades, hundreds of fluorescent proteins (FPs) have been genetically engineered to light up a variety of cutting-edge protein applications.^{3–6} However, developing a new fluorescent protein through mutagenesis is not always successful, because in most cases, the modified FPs are weakly fluorescent, or rarely shifting their colors.^{7,8} So far, only 3–5 bright FPs are frequently used for labeling and imaging proteins, and the number more than that are particularly difficult.^{9,10} In essence, the lighting mechanism of FPs is rooted in incoherent electronic transition of their chromophores, and the resulting broad fluorescence spectra (30–50 nm) physically limit the availability of resolvable colors.^{11,12} In the most recent breakthrough, 24-color Manhattan Raman Scattering (MARS) dyes possessing narrow vibrational Raman bands, exhibit an impressive advance in supermultiplex protein imaging.^{13,14} But, these superior Raman dyes still rely on traditional immune-staining procedures to target specific intracellular proteins.^{15–17} Unnatural amino acid (UAA) bearing Raman tag can be precisely incorporated into specific site of desired protein by a spare stop codon and an orthogonal aminoacyl-tRNA synthetase (aaRS)/tRNA pair.^{18–21} The attempts to construct dual-color or multicolor protein labeling using novel UAAs are being arduously explored within the traditional scope of fluorescence, but largely failed.^{22,23} The known barrier of the genetic code expansion technique is that a single UAA only responds to an amber codon, and the further color expansion via incorporation of multiple UAAs into different proteins is largely impossible.^{23–26}

The fluorescence of FPs is attributed to a large π -conjugation in the core chromophore 4-(*p*-hydroxybenzylidene)-5-imidazolinone (HBI). This chromophore structure is formed through posttranslational modifications involving three native nonfluorescent amino acids: serine 65, glycine 67 and tyrosine 66, featuring a crucial phenyl ring.²⁷ The folded β barrel in FP plays a crucial role in creating an enclosed structure for chromophore maturation, shielding self-catalyzed cyclization and oxidation reaction from bulk water and molecular oxygen.²⁸ The chromophore fluorescing, corresponding to transient electronic transition, is bright but broad in color (Figure 1a, ~46 nm in the case of pr-Kaede, full width at half-maximum, fwhm). In contrast, the molecular vibrating is significantly finer in color, corresponding to transition between vibrational bond states.^{29,30} FPs inspired us to develop genetically encoded VPs, which do not fluoresce but are engineered to vibrate strongly. To construct a VP, a correct UAA bearing an alkyne that can conjugate with the imidazolinone ring through the exocyclic C=C bridge is the key to forming a vibrating chromophore. In all engineered UAAs, we intentionally selected *p*-ethynylphenylalanine (*p*EtF), which consists of a phenyl ring and an alkynyl side group with Raman peak at 2105 cm^{-1} in the silent region.³¹ When cotransformed with a

Received: March 24, 2024

Revised: August 30, 2024

Accepted: October 4, 2024

Published: October 7, 2024



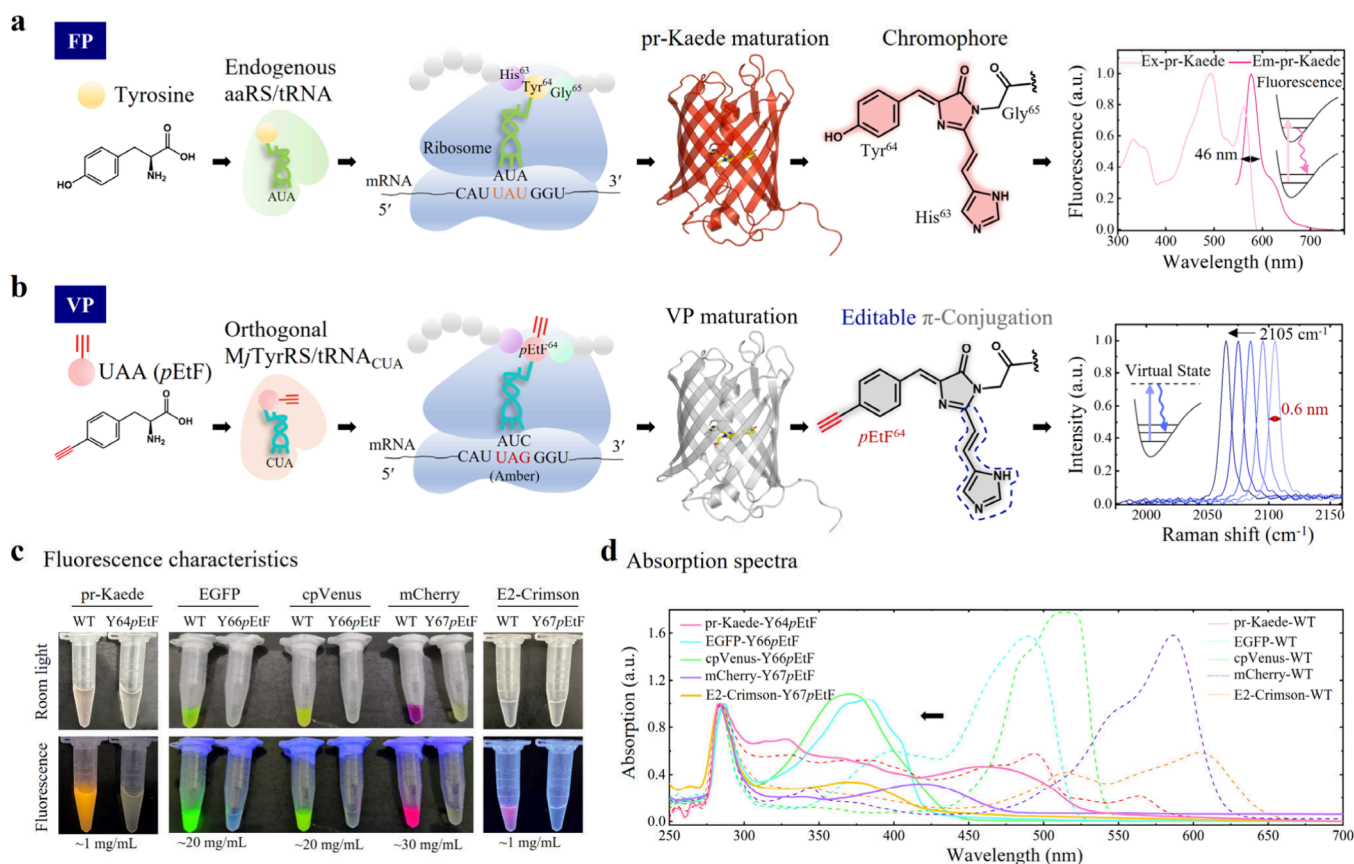


Figure 1. Concept of VP system via genetic code expansion. **a.** Translation mechanisms of the native photoconvertible FP pr-Kaede. **b.** Process of constructing VPs is based on the genetic code expansion system. From left to right: Chemical structure of tyrosine/*pEtF*, aminoacylation process of tyrosine/*pEtF*, protein translation, chromophores (depicted as stick models of photoconverted pr-Kaede-WT/pr-Kaede-Y64*pEtF*), structure of the mature chromophores formed by the His63-Tyr64-Gly65 tripeptide/the *pEtF*-incorporated VPs, and schematic excitation and emission spectra of FPs/VPs. The excitations of FPs and VPs are corresponding to electronic transition and molecular transition, respectively. **c.** Photographic pictures taken under room light (top) and irradiation of UV (~365 nm, bottom). **d.** Absorption spectra of purified FPs (pr-Kaede-WT/EGFP/cpVenus/mCherry/E2-Crimson, dashed line) and VPs (pr-Kaede/EGFP/cpVenus/mCherry/E2-Crimson-*pEtF*, solid line) prepared from *E. coli*.

pULTRA plasmid encoding aaRS/tRNA_{CUA} pair, *pEtF* can be site-specifically incorporated into a primed conversion capable (pr-) photoconvertible FP, pr-Kaede,³² but with an amber mutation at Tyr64. In particular, *pEtF* is structurally close to tyrosine and can keep on conjugating with His63 and Gly64 during chromophore maturing (it undergoes photoconversion from green to red state upon irradiation with ultraviolet or violet light).³³ As a result, the side alkynyl group of *pEtF* can cyclize with the side chain of His63 and Gly64 to form a larger π -bond conjugated structure. More importantly, analogous to the fluorescence wavelength shifting, the vibrational frequency shifting of *pEtF* allows further color expansion based on the incorporation of a single UAA and the contiguous editable amino acids (Figure 1b, blue dashed area). In this work, we engineered pr-Kaede-Y64*pEtF*, E2-Crimson-Y67*pEtF* and the other three VPs, which comprise different side chains in the chromophore. Importantly, we observed fine chromophore-enhanced Raman bands and frequency shifts of the same alkynyl group. The VPs can possibly be further reduced in size and molecular weight, potentially evolving into vibrational peptides. The proposed work paves the way for multicolor protein labeling and Raman imaging by narrow-band VPs.

RESULTS AND DISCUSSION

VP Engineering by Genetic Code Expansion. Among more than 100 UAA derivatives,^{34,35} we purposely select a phenylalanine analogue, *pEtF* (Figure 1b), which features a terminal phenyl alkyne (C≡C).³¹ In response to an encoded amber codon, *pEtF* was site-specifically incorporated into the photoconvertible fluorescent protein derived from a stony coral, pr-Kaede (chromophore: His63-Tyr64-Gly65), by means of an orthogonal *Methanococcus jannaschii* tyrosyl-tRNA synthetase/tRNA_{CUA} (MjTyrRS/tRNA_{CUA}) pair.³⁶ Specifically, a pET30a plasmid of pr-Kaede, harboring a TAG mutation at position 64 (pET30a-pr-Kaede-Y64TAG) was cotransformed with a pULTRA³⁶ plasmid of MjTyrRS/tRNA_{CUA} to express the pr-Kaede-Y64*pEtF* protein in *E. coli*. After remarkable posttranslational modifications and VP maturing, *pEtF*64 ingeniously cyclizes with His63 and Gly65 to form a larger conjugated structure encompassing a terminal alkyne, an aromatic ring, an imidazolinone, a C α =C β double bond, and an imidazole ring of histidine. Thus, the VP chromophore-enhanced alkyne possesses a sharp Raman peak about 0.6 nm (fwhm) in line width within the Raman-silent region, ~77 times narrower than the fluorescence spectrum of the corresponding FP. Over a long period, it was thought to be impossible for site-specific incorporation of a single UAA to label multiple proteins at a time. Here, by editing the

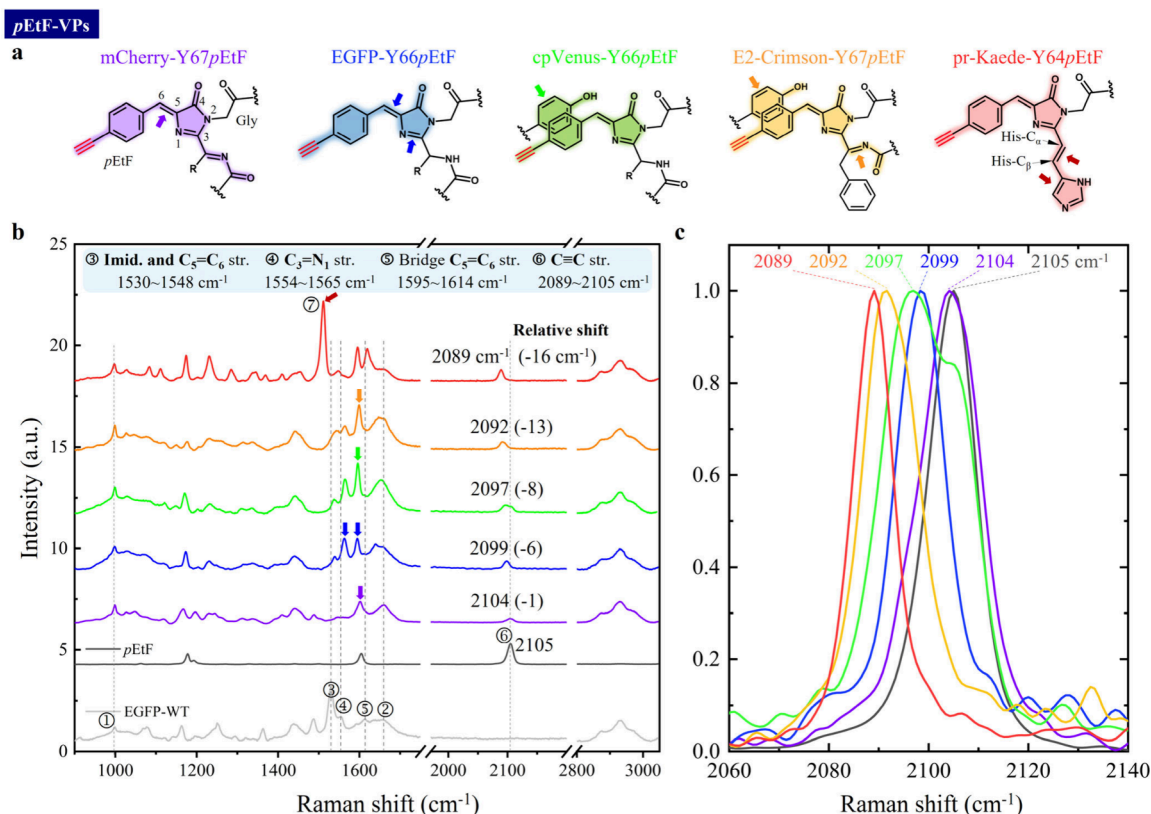


Figure 2. The Raman spectra of various *pEtF*-VPs. a. Chemical structure of chromophores in *pEtF*-incorporated VPs. Shaded areas represent the π conjugation of the newly formed chromophores. b. Raman spectra of purified VPs proteins excited at 671 nm. From bottom to top: EGFP-WT, *pEtF*, mCherry-Y67*pEtF*, EGFP-Y66*pEtF*, cpVenus-Y66*pEtF*, E2-Crimson-Y67*pEtF* and pr-Kaede-Y64*pEtF*. Characteristic Raman bands (①~⑦) of VPs were identified and assigned. ①: Benzene ring at ~ 998 cm^{-1} ; ②: Amide I band at ~ 1655 cm^{-1} ; ③: Stretch of C5 = C6 bridge, imid. C = N, new-conjugated C $_{\alpha}$ =C $_{\beta}$ bridge and C = C double bond in the His63 side chain at ~ 1510 cm^{-1} . Imid.: imidazole; Str.: Stretch. c. Zoomed-in spectra from 2060 to 2140 cm^{-1} in b.

contiguous natural amino acid residues and their conjugation with the UAA (*pEtF*64 and blue dashed area in VP chromophore, Figure 1b), we found that the narrow vibrational band of the alkyne is programmable, and the resonant frequency at 2089 cm^{-1} exhibits a significant degree of spectral shifting, which allows multicolor vibrational labeling and imaging in the future.

To prove the concept, we first engineered a series of *pEtF*-VPs, in which *pEtF* was introduced into the chromophore of pr-Kaede, EGFP, cpVenus, mCherry, and E2-Crimson, forming pr-Kaede-Y64*pEtF*, EGFP-Y66*pEtF*, cpVenus-Y66*pEtF*, mCherry-Y67*pEtF*, and E2-Crimson-Y67*pEtF*, respectively. These *pEtF*-VPs were expressed in *E. coli* at 30 °C. The highly concentrated VP solutions were obtained through Ni-NTA affinity chromatography purification, followed by dialysis and ultrafiltration with yields of soluble proteins in the range of 20–30 mg/mL (1 mg/mL before ultrafiltration). Figure 1c characterized the fluorescence properties of VPs. In contrast to their wide-type fluorescent proteins, the *pEtF*-VPs alternatives are almost colorless under room light. Moreover, the *pEtF*-VPs are not actively fluorescent and exhibit more than 10-fold reduction of fluorescence in quantum yields as they are exposed to 365 nm UV excitation. The results from sodium dodecyl sulfate-polyacrylamide gel electrophoresis (SDS-PAGE) analysis and liquid chromatography-tandem mass spectrometry (LC-MS/MS) fully confirmed the formation of the full-length proteins and the maturation of the chromophore in *pEtF*-VPs. (SDS-PAGE: Supplementary Figure S1;

LC-MS/MS: Supplementary Figure S2–6). In contrast to the fluorescent counterparts (FPs-WT), the normalized absorption spectra of all VPs show a hypsochromic shift of the main absorption bands to 365 nm in the UV range (Figure 1d). The phenomenon indicates that the electron donating ability of *pEtF* is trivial in the chromophores of VPs.³⁷ Moreover, the substantially weakened and blue-shifted fluorescence is advantageous for further Raman spectra measurements.

Raman Spectra Characterization of Various *pEtF*-VPs.

Even though the absorption bands of *pEtF*-VPs already present a hypsochromic shift back to the UV region, the excited fluorescence in 532 nm Raman is still overwhelming the vibrational spectra. 785 nm Raman with a longer excitation wavelength diminishes the fluorescence, but the Raman signal from *pEtF*-VPs is rather scarce. Thus, we constructed a 671 nm Raman system (Supplementary Figure S7) and measured Raman spectra of purified VPs, including mCherry-Y67*pEtF*, EGFP-Y66*pEtF*, cpVenus-Y66*pEtF*, E2-Crimson-Y67*pEtF* and pr-Kaede-Y64*pEtF*. Figure 2a presents the chemical structures of their chromophores, and the π -conjugation regions are intentionally highlighted in different colors. Raman spectra of pure EGFP-WT, UAA-*pEtF*, and five VPs are shown in Figure 2b. In Figure 2b, all Raman spectra were normalized by their carbon–hydrogen (CH₃) bands of protein at 2930 cm^{-1} , assuming that the chemical ratio of C \equiv C to CH₃ bonds is roughly the same for all VPs. The EGFP-WT is strongly fluorescent, but the 671 nm Raman is well suited to obtain its finer Raman spectrum (light gray). The characteristic Raman

band of benzene ring at $\sim 998\text{ cm}^{-1}$ (①) and the amide I band at $\sim 1655\text{ cm}^{-1}$ (②) due to from the main and side chain groups on the β -barrel of EGFP-WT are exhibited.^{38–40} Of greater significance, the characteristic bands of VP's chromophore, encompassing the imidazolinone ring and conjugated exocyclic C = C band at $\sim 1530\text{ cm}^{-1}$ (③), $\text{C}_3=\text{N}_1$ stretching band at $\sim 1554\text{ cm}^{-1}$ (④), and $\text{C}_5=\text{C}_6$ band at $\sim 1614\text{ cm}^{-1}$ (⑤) are also clearly exhibited and assigned. Particularly in the silent region, the stretching vibration of the $\text{C}\equiv\text{C}$ bond in UAA-*pEtF* displays a distinct sharp Raman peak at 2105 cm^{-1} (Figure 2b, dark gray, ⑥), and this terminal alkyne neither exists in the biological system nor reacts with endogenous biomolecules. Importantly, the alkyne peak of *pEtF* shifts its frequency after incorporation into different chromophores.

As *pEtF* is incorporated into the chromophore of mCherry (Met66-*pEtF*67-Gly68), the $\text{C}_5=\text{C}_6$ bond (1602 cm^{-1} , indicated by a purple arrow in Figure 2a,b) forms to bridge the *pEtF* and imidazolinone during chromophore maturation. The alkyne band of concern only slightly shifts to 2104 cm^{-1} (⑦), which is much less than what we expected. We found that the $\text{C}_5=\text{C}_6$ band at 1602 cm^{-1} was formed, but the π conjugation at $\text{C}_3=\text{N}_1$, which peaked at $\sim 1560\text{ cm}^{-1}$ (④), was very weak. It implies that *pEtF* is out of chromophore plane, hindering effective conjugation with the chromophore.⁴¹ We further constructed VP-EGFP-Y66*pEtF* (Thr65-*pEtF*66-Gly67), in which both $\text{C}_3=\text{N}_1$ and $\text{C}_5=\text{C}_6$ (~ 1563 and $\sim 1595\text{ cm}^{-1}$) bonds are more pronounced (indicated by a blue arrow in Figure 2a,b). Most importantly, the alkyne band shifted 6 cm^{-1} to the lower wavenumber (2099 cm^{-1}). VP-cpVenus-Y66*pEtF* (Gly65-*pEtF*66-Gly67, Tyr203) consists of an extra π - π stacking interactions between a Tyr ring of the chromophore and aromatic amino acids, thereby enhancing the vibration of the $\text{C}_5=\text{C}_6$ band (green arrow in Figure 2a,b), and the alkyne band further shifted 8 cm^{-1} . To enhance the hypsochromic shift, we engineered VP-E2-Crimson-Y67*pEtF* (Phe66-*pEtF*67-Gly68, Tyr197) with π conjugation extended to the second $\text{C}=\text{N}$ bond⁴² (orange arrow in Figure 2a,b), and a further 13 cm^{-1} hypsochromic shift of alkyne peak was observed. Thanks to the available abundant protein clones, we particularly constructed VP-pr-Kaede-Y64*pEtF*, in which His63-*pEtF*64-Gly65 together engaged in an interaction of β -elimination reaction, which results in a new double bond between C_α and C_β of the His63 residue, aligning the imidazole side chain in conjugation with the rest of the chromophore.⁴³ In this case, a prominent Raman band at 1510 cm^{-1} (⑧) manifested (red arrow in Figure 2a,b), which can be assigned to the successful formation of the $\text{C}_\alpha=\text{C}_\beta$ double bond in the His63 side chain.^{39,44} The alkyne peak exhibited a continuous shift of approximately 16 cm^{-1} . To make it clear, the alkyne bands of the engineered five VPs are shown in Figure 2c, and their relative Raman shifts are indicated. It suggests that the vibrational resonance of VPs is programmable by varying the adjacent amino acid residues. As shown in Supplementary Figure S8, the Raman band of pr-Kaede-Y64*pEtF* presents the strongest signal and shifts most to the lower wavenumbers. Meanwhile, mCherry-Y67*pEtF* shifts least, only 1 cm^{-1} relative to the pure *pEtF*, and gives the weakest Raman signal. Both Raman shift and intensity of alkyne largely increase with the π -conjugation degree of the chromophore. The only exception happens to cpVenus-Y66*pEtF*, which shows distinct two bands. Apparently, one alkyne peak shifts to 2097 cm^{-1} , and the other one remains

unshifted, probably due to incomplete chromophore maturation.

To explore other possible Raman bands, we tested a new UAA bearing a $\text{C}\equiv\text{N}$ bond, *para*-cyano-L-phenylalanine (*p*CNF, 2234 cm^{-1}), which is shifted 120 cm^{-1} from *pEtF* at 2105 cm^{-1} . We incorporated *p*CNF into cpVenus and E2-Crimson proteins. As shown in Supplementary Figure S9, the Raman peak shifts from 2234 to 2225 cm^{-1} and 2222 cm^{-1} , respectively. Although the observed Raman shift is much less than we expected to be, we believe that the VPs have the potential to offer broad and sharp Raman shifts for multicolor imaging in the near future.

CONCLUSIONS

In this work, we establish a method of genetic engineering of VPs via genetic code expansion, inheriting both gene targeting specificity and narrow Raman spectra. Specifically, we genetically incorporated UAA-*pEtF* into fluorescent protein chromophores containing different conjugated amino acid residues. We carried out the construction, expression, purification, and Raman spectra analysis of various Raman vibrational proteins, including EGFP-Y66*pEtF*, cpVenus-Y66*pEtF*, mCherry-Y67*pEtF*, E2-Crimson-Y67*pEtF* and pr-Kaede-Y64*pEtF*. Our efforts have successfully yielded five VPs, each exhibiting distinct Raman resonant frequencies. These results represent a significant advancement toward protein-specific VPs, potentially overcoming the "color barrier".

ASSOCIATED CONTENT

Supporting Information

The Supporting Information is available free of charge at <https://pubs.acs.org/doi/10.1021/acs.analchem.4c01569>.

The introduction of 671 nm laser confocal Raman spectroscopy system, experimental materials, methods, and additional references (PDF)

AUTHOR INFORMATION

Corresponding Authors

Wei Chen – Britton Chance Center and MoE Key Laboratory for Biomedical Photonics, Wuhan National Laboratory for Optoelectronics-Huazhong University of Science and Technology, Wuhan, Hubei 430074, China; orcid.org/0000-0001-5567-7463; Email: w.chen@hust.edu.cn

Chun Tang – Beijing National Laboratory for Molecular Sciences, College of Chemistry and Molecular Engineering, PKU-Tsinghua Center for Life Science, Center for Quantitative Biology, Academy for Advanced Interdisciplinary Studies, Peking University, Beijing 100871, China; orcid.org/0000-0001-6477-6500; Email: Tang_Chun@pku.edu.cn

Ping Wang – Britton Chance Center and MoE Key Laboratory for Biomedical Photonics, Wuhan National Laboratory for Optoelectronics-Huazhong University of Science and Technology, Wuhan, Hubei 430074, China; Changping Laboratory, Beijing 102206, China; Huaiyin Institute of Technology, Huaian, Jiangsu 223003, China; orcid.org/0000-0002-5168-6829; Email: p_wang@hust.edu.cn

Authors

Yage Chen – Britton Chance Center and MoE Key Laboratory for Biomedical Photonics, Wuhan National Laboratory for Optoelectronics-Huazhong University of Science and

Technology, Wuhan, Hubei 430074, China; orcid.org/0000-0002-6601-5198

Zhiliang Huang – Britton Chance Center and MoE Key Laboratory for Biomedical Photonics, Wuhan National Laboratory for Optoelectronics-Huazhong University of Science and Technology, Wuhan, Hubei 430074, China; Changping Laboratory, Beijing 102206, China

Erli Cai – Britton Chance Center and MoE Key Laboratory for Biomedical Photonics, Wuhan National Laboratory for Optoelectronics-Huazhong University of Science and Technology, Wuhan, Hubei 430074, China

Shuchen Zhong – Beijing National Laboratory for Molecular Sciences, College of Chemistry and Molecular Engineering, PKU-Tsinghua Center for Life Science, Center for Quantitative Biology, Academy for Advanced Interdisciplinary Studies, Peking University, Beijing 100871, China

Haozheng Li – Changping Laboratory, Beijing 102206, China

Wei Ju – Britton Chance Center and MoE Key Laboratory for Biomedical Photonics, Wuhan National Laboratory for Optoelectronics-Huazhong University of Science and Technology, Wuhan, Hubei 430074, China; Changping Laboratory, Beijing 102206, China

Jie Yang – Britton Chance Center and MoE Key Laboratory for Biomedical Photonics, Wuhan National Laboratory for Optoelectronics-Huazhong University of Science and Technology, Wuhan, Hubei 430074, China

Complete contact information is available at:

<https://pubs.acs.org/10.1021/acs.analchem.4c01569>

Author Contributions

¹Y.G.C., Z.L.H. and E.L.C. contributed equally.

Notes

The authors declare no competing financial interest.

ACKNOWLEDGMENTS

P.W. acknowledges the supports from the National Natural Science Foundation of China (62075076), Science Fund for Creative Research Group of China (61421064), and Innovation Fund of the Wuhan National Laboratory for Optoelectronics. W.C. acknowledges the support from the National Natural Science Foundation of China (22277032). The authors thank the support from Analytical and Testing Center (HUST) and the Optical Bioimaging Core Facility of WNLO-HUST.

REFERENCES

- (1) Tsien, R. Y. *Annu. Rev. Biochem.* **1998**, *67*, 509–44.
- (2) Chalfie, M. *Angew. Chem., Int. Ed. Engl.* **2009**, *48* (31), 5603–11.
- (3) Dean, K. M.; Palmer, A. E. *Nat. Chem. Biol.* **2014**, *10* (7), 512–523.
- (4) Hirano, M.; Ando, R.; Shimozono, S.; Sugiyama, M.; Takeda, N.; Kurokawa, H.; Deguchi, R.; Endo, K.; Haga, K.; Takai-Todaka, R.; Inaura, S.; Matsumura, Y.; Hama, H.; Okada, Y.; Fujiwara, T.; Morimoto, T.; Katayama, K.; Miyawaki, A. *Nat. Biotechnol.* **2022**, *40* (7), 1132–1142.
- (5) Zhang, S.; Ai, H. W. *Nat. Chem. Biol.* **2020**, *16* (12), 1434–1439.
- (6) Zhang, H. B.; Papadaki, S.; Sun, X. T.; Wang, X. Y.; Drobizhev, M.; Yao, L. X.; Rehbock, M.; Koster, R. W.; Wu, L. F.; Namikawa, K.; Piatkevich, K. D. *Nat. Meth.* **2023**, *20*, 1605–1616.
- (7) Aarthy, M.; George, A.; Ayyadurai, N. *Int. J. Biol. Macromol.* **2021**, *191*, 840–851.
- (8) Nienhaus, K.; Nienhaus, G. U. *Chem. Soc. Rev.* **2014**, *43* (4), 1088–1106.
- (9) Valm, A. M.; Cohen, S.; Legant, W. R.; Melunis, J.; Hershberg, U.; Wait, E.; Cohen, A. R.; Davidson, M. W.; Betzig, E.; Lippincott-Schwartz, J. *Nature* **2017**, *546* (7656), 162–167.
- (10) Shou, J. W.; Oda, R.; Hu, F. H.; Karasawa, K.; Nuriya, M.; Yasui, M.; Shiramizu, B.; Min, W.; Ozeki, Y. *Iscience* **2021**, *24* (8), 102832.
- (11) Lakowicz, J. R. *Principles of fluorescence spectroscopy*, 3rd ed.; Springer, 2006; p xxvi.
- (12) Giepmans, B. N. G.; Adams, S. R.; Ellisman, M. H.; Tsien, R. Y. *Science* **2006**, *312* (5771), 217–224.
- (13) Wei, L.; Chen, Z.; Shi, L.; Long, R.; Anzalone, A. V.; Zhang, L.; Hu, F.; Yuste, R.; Cornish, V. W.; Min, W. *Nature* **2017**, *544* (7651), 465–470.
- (14) Miao, Y. P.; Qian, N. X.; Shi, L. X.; Hu, F. H.; Min, W. *Nat. Commun.* **2021**, *12* (1), 4518.
- (15) Hu, F.; Zeng, C.; Long, R.; Miao, Y.; Wei, L.; Xu, Q.; Min, W. *Nat. Methods* **2018**, *15* (3), 194–200.
- (16) Qian, N. X.; Min, W. *Curr. Opin. Chem. Biol.* **2022**, *67*, 102115–102126.
- (17) Zhao, Z. L.; Chen, C.; Wei, S. X.; Xiong, H. Q.; Hu, F. H.; Miao, Y. P.; Jin, T. W.; Min, W. *Nat. Commun.* **2021**, *12* (1), 1305.
- (18) Zhang, J.; Yan, S.; He, Z.; Ding, C.; Zhai, T.; Chen, Y.; Li, H.; Yang, G.; Zhou, X.; Wang, P. *J. Phys. Chem. Lett.* **2018**, *9* (16), 4679–4685.
- (19) Baumann, T.; Hauf, M.; Schildhauer, F.; Eberl, K. B.; Durkin, P. M.; Deniz, E.; Löffler, J. G.; Acevedo-Rocha, C. G.; Jaric, J.; Martins, B. M.; Dobbek, H.; Bredenbeck, J.; Budisa, N. *Angew. Chem., Int. Ed.* **2019**, *58* (9), 2899–2903.
- (20) de la Torre, D.; Chin, J. W. *Nat. Rev. Genet.* **2021**, *22* (3), 169–184.
- (21) Butler, N. D.; Sen, S.; Brown, L. B.; Lin, M. W.; Kunjapur, A. M. *Nat. Chem. Biol.* **2023**, *19* (7), 911–920.
- (22) Elia, N. *FEBS J.* **2021**, *288* (4), 1107–1117.
- (23) Zheng, Y.; Addy, P. S.; Mukherjee, R.; Chatterjee, A. *Chem. Sci.* **2017**, *8* (10), 7211–7217.
- (24) Saal, K.-A.; Richter, F.; Rehling, P.; Rizzoli, S. O. *ACS Nano* **2018**, *12* (12), 12247–12254.
- (25) Dunkelmann, D. L.; Willis, J. C. W.; Beattie, A. T.; Chin, J. W. *Nat. Chem.* **2020**, *12* (6), 535–544.
- (26) Italia, J. S.; Addy, P. S.; Erickson, S. B.; Peeler, J. C.; Weerapana, E.; Chatterjee, A. *J. Am. Chem. Soc.* **2019**, *141* (15), 6204–6212.
- (27) Hu, C.; Liu, X.; Wang, J. *Science* **2020**, *367* (6473), 26.
- (28) Stepanenko, O. V.; Stepanenko, O. V.; Kuznetsova, I. M.; Verkhusa, V. V.; Turoverov, K. K. *Int. Rev. Cell Mol. Biol.* **2013**, *302*, 221–78.
- (29) Cheng, J. X.; Xie, X. S. *Science* **2015**, *350* (6264), aaa8870.
- (30) Hu, F. H.; Shi, L. X.; Min, W. *Nat. Meth.* **2019**, *16* (9), 830–842.
- (31) Miyake-Stoner, S. J.; Miller, A. M.; Hammill, J. T.; Peeler, J. C.; Hess, K. R.; Mehl, R. A.; Brewer, S. H. *Biochemistry* **2009**, *48* (25), 5953–5962.
- (32) Mohr, M. A.; Kobitski, A. Y.; Sabater, L. R.; Nienhaus, K.; Obara, C. J.; Lippincott-Schwartz, J.; Nienhaus, G. U.; Pantazis, P. *Angew. Chem., Int. Ed.* **2017**, *56* (38), 11628–11633.
- (33) Mizuno, H.; Mal, T. K.; Tong, K. I.; Ando, R.; Furuta, T.; Ikura, M.; Miyawaki, A. *Mol. Cell* **2003**, *12* (4), 1051–8.
- (34) Dumas, A.; Lercher, L.; Spicer, C. D.; Davis, B. G. *Chem. Sci.* **2015**, *6* (1), 50–69.
- (35) Nodding, A. R.; Spear, L. A.; Williams, T. L.; Luk, L. Y. P.; Tsai, Y. H. *Essays Biochem.* **2019**, *63* (2), 237–266.
- (36) Schultz, K. C.; Supekova, L.; Ryu, Y. H.; Xie, J. M.; Perera, R.; Schultz, P. G. *J. Am. Chem. Soc.* **2006**, *128* (43), 13984–13985.
- (37) Wang, L.; Xie, J.; Deniz, A. A.; Schultz, P. G. *J. Org. Chem.* **2003**, *68* (1), 174–6.
- (38) Yuan, Y.; Wang, D.; Zhang, J.; Liu, J.; Chen, J.; Zhang, X. E. *Biophys. Rep.* **2018**, *4* (5), 265–272.

(39) Chen, C.; Henderson, J. N.; Ruchkin, D. A.; Kirsh, J. M.; Baranov, M. S.; Bogdanov, A. M.; Mills, J. H.; Boxer, S. G.; Fang, C. *Int. J. Mol. Sci.* **2023**, *24* (15), 11991.

(40) Fang, C.; Frontiera, R. R.; Tran, R.; Mathies, R. A. *Nature* **2009**, *462* (7270), 200–4.

(41) Subach, F. V.; Verkhusha, V. V. *Chem. Rev.* **2012**, *112* (7), 4308–4327.

(42) Strack, R. L.; Hein, B.; Bhattacharyya, D.; Hell, S. W.; Keenan, R. J.; Glick, B. S. *Biochemistry* **2009**, *48* (35), 8279–81.

(43) Yampolsky, I. V.; Kislukhin, A. A.; Amatov, T. T.; Shcherbo, D.; Potapov, V. K.; Lukyanov, S.; Lukyanov, K. A. *Bioorg. Chem.* **2008**, *36* (1–3), 96–104.

(44) Krueger, T. D.; Tang, L. T.; Zhu, L. D.; Breen, I. L.; Wachter, R. M.; Fang, C. *Angew. Chem., Int. Ed.* **2020**, *59* (4), 1644–1652.